European Journal of Radiology Open 3 (2016) 16–21

Contents lists available at ScienceDirect

European Journal of Radiology Open

journal homepage: www.elsevier.com/locate/ejro

Staging of pelvic lymph nodes in patients with prostate cancer: Usefulness of multiple *b* value SE-EPI diffusion-weighted imaging on a 3.0 T MR system

Valentina Vallini[a], Simona Ortori[a], Piero Boraschi[a], Francesca Manassero[b], Michela Gabelloni[a], Lorenzo Faggioni[a,*], Cesare Selli[b], Carlo Bartolozzi[a]

[a] Department of Diagnostic and Interventional Radiology, University of Pisa, Via Paradisa 2, 56124 Pisa, Italy
[b] Department of Urology, University of Pisa, Via Paradisa 2, 56124 Pisa, Italy

ARTICLE INFO

Article history:
Received 22 November 2015
Accepted 24 November 2015
Available online 11 December 2015

Keywords:
Diffusion-weighted MR imaging
3 T system
Lymph nodes
Prostate cancer

ABSTRACT

Purpose: To evaluate the usefulness of diffusion-weighted imaging (DWI) with a multiple *b* value SE-EPI sequence on a 3.0 T MR scanner for staging of pelvic lymph nodes in patients with prostate cancer candidate to radical prostatectomy and extended pelvic lymph node dissection (PLND).
Materials and methods: Institutional review board approval was obtained and written informed consent was taken from all enrolled subjects. A series of 26 patients with pathologically proven prostate cancer (high or intermediate risk according to D'Amico risk groups) scheduled for radical prostatectomy and PLND underwent 3 T MRI before surgery. DWI was performed using an axial respiratory-triggered spin-echo echo-planar sequence with multiple *b* values (500, 800, 1000, 1500 s/mm^2) in all diffusion directions. ADC values were calculated by means of dedicated software fitting the curve obtained from the corresponding ADC for each *b* value. Fitted ADC measurements were performed at the level of proximal and distal external iliac, internal iliac, and obturator nodal stations bilaterally. Lymph node appearance was also assessed in terms of short axis, long-to-short axis ratio, node contour and intranodal heterogeneity of signal intensity.
Results: A total of 173 lymph nodes and 104 nodal stations were evaluated on DWI and pathologically analysed. Mean fitted ADC values were $0.79 \pm 0.14 \times 10^{-3}$ mm^2/s for metastatic lymph nodes and $1.13 \pm 0.29 \times 10^{-3}$ mm^2/s in non-metastatic ones ($P < 0.0001$). The cut-off for fitted ADC obtained by ROC curve analysis was 0.91×10^{-3} mm^2/s. A two-point-level score was assigned for each qualitative parameter, and the mean grading score was 6.09 ± 0.61 for metastastic lymph nodes and 5.42 ± 0.79 for non-metastatic ones, respectively ($P = 0.001$). Using a score threshold of 4 for morphological, structural, and dimensional MRI analysis and a cut--off value of 0.91×10^{-3} mm^2/s for fitted ADC measurements of pelvic lymph nodes, per--station sensitivity, specificity, PPV, NPV and diagnostic accuracy were 100%, 7.9%, 15.6%, 100% and 21.3%, and 84.6%, 89.5%, 57.9%, 97.1% and 88.8%, respectively.
Conclusions: 3.0T DWI with a multiple *b* value SE-EPI sequence may help distinguish benign from malignant pelvic lymph nodes in patients with prostate cancer.

1. Introduction

The presence of pelvic lymph node metastases in patients with prostate cancer is of major relevance since it is crucial for treatment planning. Currently, pelvic lymph node dissection (PLND) represents the most accurate and reliable staging procedure for the detection of lymph node invasion in prostate cancer, but not all patients are at the same risk of harboring pelvic lymph node metastases [1]. Radical prostatectomy with PLND is a time-consuming and relatively expensive procedure that requires inpatient hospitalization and is associated with potentially early post-operative complications (such as bleeding, infections, lymphocele) and late post-operative complications (e.g., urinary incontinence, erectile dysfunction, anastomotic stenosis). For this reason, non-invasive imaging is important to streamline the surgical resection protocol and has a potential role in selecting patients who are suitable for PLND [2,3].

* Corresponding author.
E-mail address: lfaggioni@sirm.org (L. Faggioni).

http://dx.doi.org/10.1016/j.ejro.2015.11.004

Table 1
D'Amico risk groups.

High risk	PSA* > 20 or Gleason ≥ 8 or are in clinical stage T2c-3a
Intermediate risk	Gleason score of 7 or PSA of 10–20 or are in clinical stage T2b
Low risk	PSA ≤ 10 ng/ml and Gleason score ≤ 6 or are in clinical stage T1-2a

PSA* = prostate-specific antigen, expressed in ng/ml.

Nodal staging is routinely performed by cross-sectional imaging such as computed tomography (CT) and is based on the morphological and dimensional features of lymph nodes, including their size (with a threshold of 10 mm in short axis diameter or clusters of smaller regional lymph nodes), long-to-short axis ratio, borders (lobulated or spiculated), extra-capsular spread, and abnormal internal architecture (such as central necrosis) [4,5].

MR diffusion-weighted imaging (DWI) is a non-invasive imaging technique yielding unique information on molecular diffusion properties of tissues. DWI allows to evaluate the random thermal motion of water molecules (Brownian motion), which is generally limited in cancer tissues because of their relatively high cell density and abundance of cellular membranes as compared to normal tissues. The mobility of water molecules is quantified by the apparent diffusion coefficient (ADC) [4]. Conventionally, restricted water diffusion in areas of high cellular density (e.g., tumors) results in low ADC values compared with areas with lower cellular density, which typically show higher ADC values.

As to the differential diagnosis between benign and malignant lymph nodes with DWI, the high signal intensity of lymph nodes in high *b* value images must not be misinterpreted, because also reactive nodal hyperplasia can result in increased cellularity and thus high signal intensity on DWI images [4]. In clinical practice, DWI of lymph nodes is performed using high *b* values to increase the conspicuity of high cellularity lymph nodes [6], and in this setting at least two or more *b* values are used for DWI analysis. In light of the above assumptions, quantitative evaluation of ADC maps might provide useful information for presurgical assessment of pelvic lymph nodes, which however needs to be interpreted with caution [4].

The purpose of our study was to evaluate the usefulness of DWI with a multiple *b* value spin-echo echo-planar (SE-EPI) sequence on a 3.0 T MR scanner for staging of pelvic lymph nodes in patients with prostate cancer candidate to radical prostatectomy and extended PLND.

2. Materials and methods

2.1. Patients population

Between June 2011 and November 2013, a series of 26 patients (median age 66.3 ± 6.7 years, range 49–76 years) with pathologically proven prostate cancer (high or intermediate risk according to D'Amico risk groups; Table 1) scheduled for radical prostatectomy and PLND underwent MRI before surgery. Exclusion criteria were the following: known bone metastases, previous treatment for prostate cancer, previous/concomitant malignancy, and contraindications to MRI.

All patients were examined on a 3.0 T MRI scanner (Discovery MR750; GE Healthcare, Milwaukee, WI) using a phased array 8-channel surface coil (gradient field strength 50 mT/m, slew rate 200 T/m/s). Institutional review board approval was obtained, and a written informed consent was obtained from all enrolled patients after the nature of the procedure had been fully explained.

All patients underwent radical prostatectomy within 15 days of MRI. Lymph nodes were surgically mapped and classified into ten different anatomic regions (proximal and distal external iliac, proximal and distal internal iliac, and obturator, each on both the right and left sides).

Table 2
Demographic and biometric information (patients *n* = 26).

Patients, *N*	26
Age, mean (range)	66.3 (49–76)
Preoperative PSA, mean (range)	14.8 (3–40.6)
Biopsy Gleason grade	
6 (3 + 3)	2
7 (3 + 4)	7
7 (4 + 3)	6
8 (4 + 4)	5
9 (4 + 5)	4
9 (5 + 4)	2
Dissected lymph nodes, *n*	442
Lymph node count, mean (range)	17 (7–32)
Dissected nodal stations, *n*	212
Metastatic nodal stations, *n*/N (%)	21/212 (9.9)
Non-metastatic nodal stations, *n*/N (%)	191/212 (90.1)

In 6 out of 26 patients (23%), extended lymphadenectomy including the ten above-mentioned nodal stations was performed, while in the remaining 20 patients (77%) all ten nodal stations were not completely removed at the surgeon's discretion, since lymphadenectomy was not extended to stations where lymph nodes were neither evident on MRI nor intraoperatively visible or palpable. A total of 212 nodal stations, corresponding to 442 lymph nodes (median 17 lymph nodes per patient, range 7–32 per patient), were surgically removed and pathologically analysed. A pathologist with more than 15 years of experience in urogenital pathology was responsible for assessing all pathological specimens, and received an anatomical template marking the dissected nodal stations. However, if no nodes were found, the entire tissue underwent pathological analysis.

Demographic and biometric data of the study group are summarised in Table 2.

2.2. MR image acquisition protocol and analysis

The entire pelvis spanning from the aortic bifurcation to the pubic symphysis was imaged by performing, as a first step, a fast spin echo (FSE) T1-weighted sequence (TR 600–800 ms, TE 6–7 ms; slice section 4 mm, spacing 0.4 mm, matrix 320 × 320, 3 Nex) and subsequently, a FSE T2-weighted sequence (TR 5000–8000 ms, TE 80–85 ms, slice section 4 mm; spacing 0.4 mm, matrix 384 × 352, 4 Nex) acquired in the transverse and coronal planes.

DWI was performed using an axial respiratory-triggered SE-EPI sequence with multiple *b* values (500, 800, 1000, 1500 s/mm^2) in all diffusion directions. Imaging parameters were the following: TR (repetition time automatically adapted to the patient's breathing pattern) 3500–9200 ms, TE 65–69 ms, slice section 4 mm, spacing 0.4 mm, matrix 96 × 224, 4 Nex. The acquisition time for the whole MRI examination ranged from 25 to 30 min. The multiple *b* value DWI acquisition lasted no more than 6 min overall.

MR images were analysed in consensus by two radiologists with more than 15 years of experience in urogenital imaging and MRI, who were blinded to patient-related information such as patient identification data, history or final diagnosis. Lymph nodes were identified on T2-weighted FSE images and classified into ten different stations, as described in Section 2.1.

The features of pelvic lymph nodes on the FSE MR images were assessed in terms of their short axis, long-to-short axis ratio, node contour, and heterogeneity of intranodal signal intensity. To quantify each of these parameters, a grading score (Table 3) was assigned based on a two-point-level system, and the global grading of each nodal station was obtained by summing the point-level obtained for each of the following four parameters:

Table 3
Grading score system.

	1 point	2 points
Intranodal signal intensity	Homogeneous	Inhomogeneous
Short axis	≤10 mm	>10 mm
Nodal contour	Regular	Irregular
Long-to-short axis ratio	≥2	<2

1. Short axis ≤ 10 mm (1 point) or > 10 mm (2 points)
2. Long-to-short axis ratio ≥ 2 (1 point) or < 2 (2 points)
3. Regular (1 point) or irregular node contour (2 points)
4. Homogeneous (1 point) or inhomogeneous intranodal signal intensity (2 points).

Consequently, the global Grading Score ranged between 4 (indicator of a benign nature) and 8, i.e., the worst score indicator of a malignant nature.

The ADC values of pelvic lymph nodes were calculated on a dedicated workstation (Advantage Windows 4.5, GE Healthcare, Milwaukee, WI). All ADC measurements were obtained from the multiple *b* value SE-EPI DWI sequence by means of dedicated software fitting the curve obtained from the corresponding ADC for each *b* value. To calculate fitted ADC values, regions of interest (ROIs) were placed in lymph nodes by another radiologist with 5 years of experience in abdominal imaging and MRI, who was blinded to patient information including clinical history, previous radiological findings, and final diagnosis. To measure fitted ADC values, care was taken to place three ROIs as similar as possible inside each lymph node. In order to maximize the reproducibility of measurements, circular ROIs were chosen to sample the largest possible area within pelvic lymph nodes. To avoid errors due to partial volume averaging, ROIs not smaller than 30 mm^2 were traced, and nodes smaller than 5 mm in their largest diameter were excluded from quantitative analysis.

For each fitted ADC value, we obtained three ADC measurements and considered their average value. Likewise, in nodal stations comprising multiple lymph nodes we measured the fitted ADC value of every lymph node and considered their average value.

2.3. Statistical analysis

Statistical analysis was carried out using commercially available statistical software (MedCalc version 12.6.1.0, www.medcalc.org).

The distribution of qualitative variables was expressed as the relative frequency of the various modalities under observation, while the distribution of quantitative variables was expressed as mean, standard deviation, minimum, maximum, and number of observations.

The two-tailed Student's *t* test was used to compare the fitted ADC values measured at nodal stations in the metastatic and non-metastatic lymph node groups. The global Grading Scores in the two groups were compared using the two-tailed Mann–Whitney test. A *P* value less than 0.05 was set as threshold for statistical significance.

To evaluate the diagnostic performance of the fitted ADC in differentiating metastatic from non-metastatic lymph nodes, receiver operating characteristic (ROC) curve analysis was performed to extract the optimal threshold yielding the best separation between them. Sensitivity, specificity, positive predictive value (PPV), negative predictive value (NPV) and diagnostic accuracy were calculated both for the fitted ADC values and the global grading score.

Table 4
Location of pelvic nodal stations and number of lymph nodes per station analysed.

Pelvic nodal stations	No.	No. of lymph nodes
Right proximal external iliac	16	34
Left proximal external iliac	7	12
Right distal external iliac	16	29
Left distal external iliac	13	26
Right proximal internal iliac	8	10
Left proximal internal iliac	1	1
Right distal internal iliac	4	4
Left distal internal iliac	5	7
Right obturator	14	17
Left obturator	19	32
Right common iliac	1	1
Left common iliac	0	0
Total	104	173

3. Results

All patients tolerated the MR examination well and were able to complete the MR protocol.

Imaging analysis was limited to 104 nodal stations for a total of 173 lymph nodes, since only nodes with a maximum diameter not smaller than 5 mm and available pathological diagnosis were included. All remaining lymph nodes in the various pelvic nodal stations were not considered and therefore excluded from analysis. Location of the pelvic nodal stations and the number of lymph nodes per station analysed are reported in Table 4.

The mean global grading score was 6.09 ± 0.61 (range 5–7) in the metastatic node group and 5.42 ± 0.79 (range 4–7) in the non-metastatic node group ($P = 0.001$). A Grading Score equal to 4 (highly indicative of a benign nature) was found in 6/85 nodal stations only of the non-metastatic node group, while the remaining 79 nodal stations showed a grading score greater than 4 (a total grading score > 4 was considered suspicious for malignancy). In the metastatic node group, all nodal stations showed a grading score greater or equal than 5. All lymph nodes in the metastatic node group detected on FSE images were smaller than 10 mm in their short axis, and one patient had a benign lymph node larger than 10 mm (13.5 mm) in its short axis.

With a score threshold of 4, per-station sensitivity, specificity, PPV, NPV and diagnostic accuracy for FSE-MRI analysis were 100%, 7.9%, 15.6%, 100% and 21.3%, respectively.

The mean fitted ADC value was $0.79 \pm 0.14 \times 10^{-3}$ mm^2/s in the metastatic node group and $1.13 \pm 0.29 \times 10^{-3}$ mm^2/s in the non-metastatic node group ($P < 0.0001$).

Mean total Grading Scores and mean fitted ADC values in the two different lymph node groups are reported in Table 5. Examples of findings related to benign and malignant lymph nodes are illustrated in Figs. 1–3 .

The area under the ROC curve related to the ADC difference between the metastatic and non-metastatic node groups was 0.89 (Fig. 4). The ADC threshold value yielding the best separation between metastatic and non-metastatic lymph nodes as determined by ROC curve analysis was 0.91×10^{-3} mm^2/s. Accordingly,

Table 5
Mean total grading score and mean fitted ADC values in the two different groups of pelvic lymph nodes.

	Pathologically metastatic	Pathologically benign	*P* value
No. of nodal stations	19	85	
ADC value*	0.79 ± 0.14	1.13 ± 0.29	<0.0001
(Mean ± SD, range)	0.63–1.12	0.10–2.20	
Global grading score	6.09 ± 0.61	5.42 ± 0.79	0.001
(Mean ± SD, range)	5–7	4–7	

* Values expressed as 10^{-3} mm^2/s. SD = standard deviation.

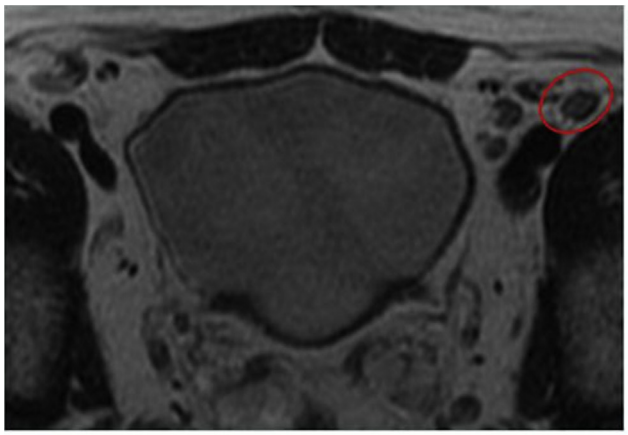

a.

	Point 1	Point 2
Intranodal signal intensity (SI)		Heterogeneous
Short axis	≤10mm	
Nodal contour	Regular	
L/S Ratio		<2

d.

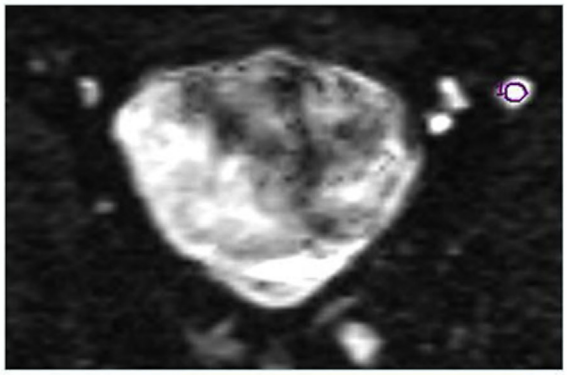

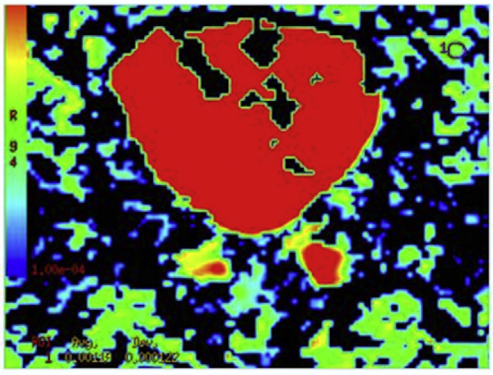

b. ADC 1,19 x 10 $^{-3}$ mm ^{2} /s → Follicular hyperplasia c.

Fig. 1. An example of benign lymph node. (a) T2w image. (b) DW image. (c) ADC map. (d) Grading score = 6.

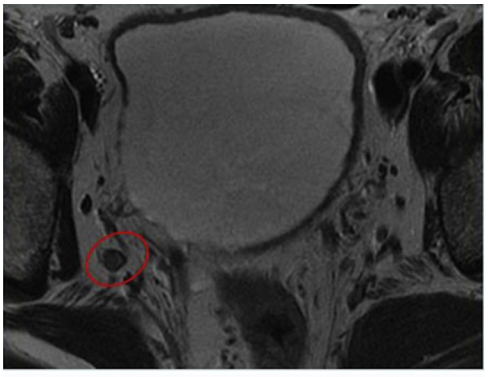

a.

	Point 1	Point 2
Intranodal signal intensity (SI)		Heterogeneous
Short axis	≤10mm	
Nodal contour		Irregular
L/S Ratio		<2

d.

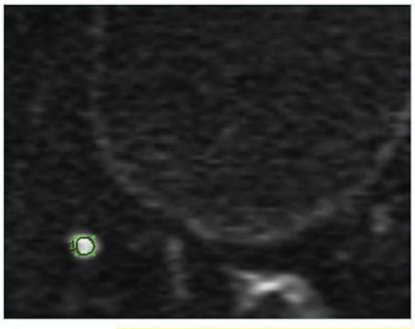

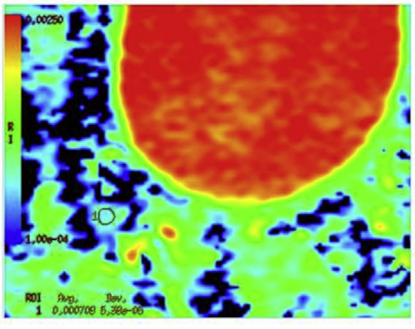

b. ADC 7,09 x 10 $^{-4}$ mm ^{2} /s → metastatic c.

Fig. 2. An example of metastatic lymph node. (a) T2w image. (b) DW image. (c) ADC map. (d) Grading score = 7.

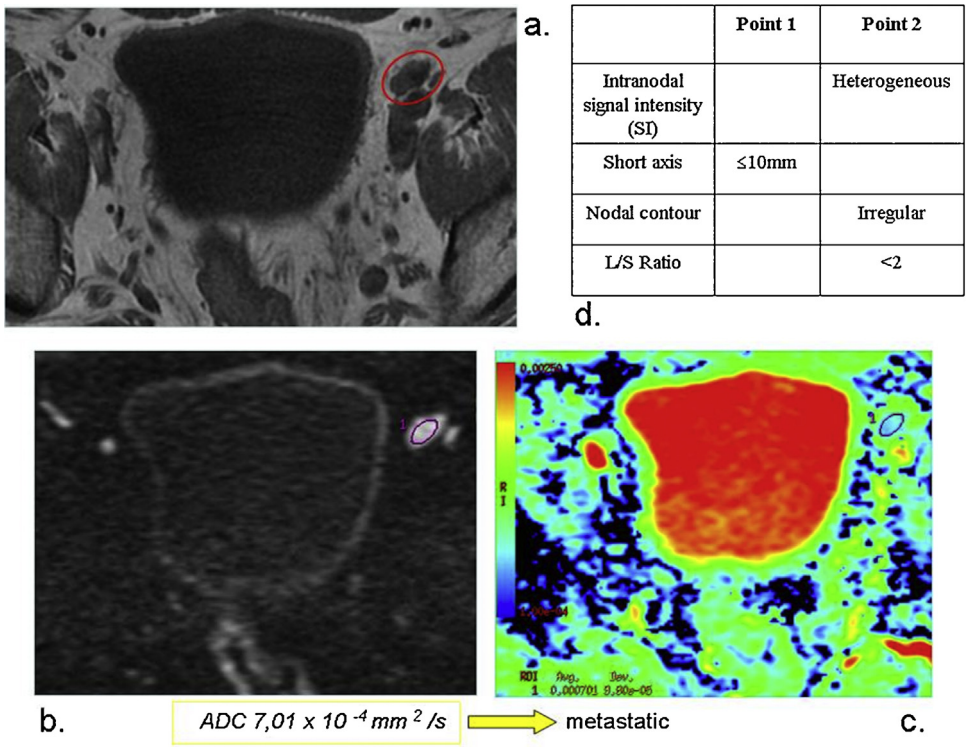

Fig. 3. Another example of metastatic lymph node. (a) T2w image. (b) DW image. (c) ADC map. (d) Grading score = 7.

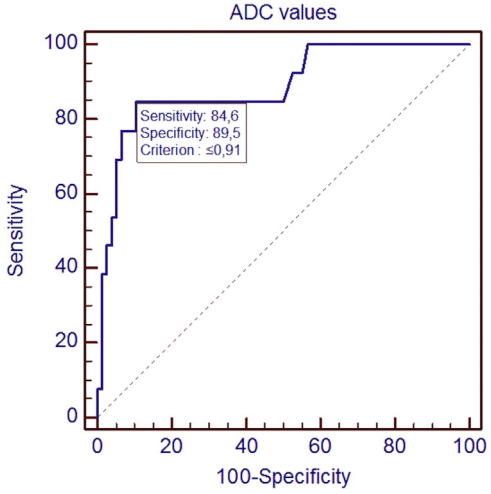

Fig. 4. The receiver operating curve (ROC) analysis showed an area under the curve (AUC) of 0.89.

a fitted ADC value equal to or less than 0.91×10^{-3} mm^2/s was considered to be associated with lymph node metastasis (Table 6).

Finally, per-station sensitivity, specificity, PPV, NPV values and diagnostic accuracy for DWI analysis were 84.6%, 89.5%, 57.9%, 97.1% and 88.8%, respectively.

Table 6
MRI findings according to the apparent diffusion coefficient (ADC) map per nodal station ($n = 104$).

ADC value	Positive pathological specimen
$\leq 0.91 \times 10^{-3}$ mm^2/s	15
$>0.91 \times 10^{-3}$ mm^2/s	4

4. Discussion

Preoperative detection of lymph node metastases in patients with prostate cancer is crucial for selection of the appropriate treatment strategy and is therefore relevant for patient prognosis. Some authors favor performing PLND in all patients who are candidates for radical prostatectomy, regardless of baseline tumor characteristics [7]. Nevertheless, the staging benefit is balanced by the risk of exposing a certain number of patients to significant and potentially unnecessary PLND-related complications. Conventional cross-sectional imaging techniques such as CT cannot accurately differentiate between benign and malignant lymph nodes, especially in the case of smaller nodes (<10 mm), so that smaller metastases often go undetected. Similarly, standard MRI, dynamic contrast-enhanced MRI, and even MR spectroscopic imaging have shown no advantage over CT in predicting metastatic involvement of lymph nodes [8,9]. Indeed, recent studies have shown that meticulous lymph node dissection in patients with prostate cancer discloses a rate of metastases as high as 25% in patients with preoperatively negative standard imaging studies [10]. The use of lymphotropic ultrasmall superparamagnetic particles of iron oxide (USPIO) as MRI contrast agents has been evaluated as well. In a study including 80 men with clinically localized prostate cancer, this technique has shown to increase the sensitivity for detection of lymph node metastases from 35% when using MRI alone to 90% [11]. However, image interpretation is time-consuming, since a node-by-node comparison must be made between pre- and post-contrast MRI images, and requires special expertise. Moreover, this technique cannot overcome the problem of false-negative normal-sized lymph nodes harboring micrometastases, and USPIO agents are not available in the daily clinical practice [11]. However, the combination of DWI and USPIO has yielded interesting results [12]. In fact, in normal lymph nodes, the uptake of iron oxide particles by the reticuloendothelial system produces a signal decrease on T2/T2*-weighted images, while malignant lymph nodes show high signal intensity due to the combination of the two effects (i.e., reduced dif-

fusion together with relatively unchanged T2/T2* following USPIO administration), resulting in better separation from normal lymph nodes, which are supposed to become invisible due to the reduced T2/T2*.

Lymph node assessment with DWI is currently one of the most interesting fields of research in oncological imaging, and ADC is a quantitative parameter that reflects the diffusion of water and tissue perfusion. In particular, DWI has been investigated as a potential tool to differentiate benign from malignant lymph nodes in head and neck cancer [13]. A large spectrum of ADC values among metastatic lymph nodes was found and can be explained by differences in the cellular composition of tumors. When comparing ADC values for any organ and lesion reported in the literature, attention has also to be paid to the choice of the underlying *b* value, on which ADC is strongly dependent [14].

Based on our preliminary findings, DWI may help distinguish benign from malignant lymph nodes in patients with prostate cancer, since fitted ADC value of metastatic lymph nodes were significantly lower than those of non-metastatic lymph nodes with a NPV as high as 97.1%.

As to the morphological, structural, and dimensional MRI analysis of pelvic lymph nodes, we found a significant difference between the total Grading Score in the metastatic and non-metastatic node groups, yet very low specificity, PPV and diagnostic accuracy were observed. We also found that the mean diameter (short axis) of metastatic lymph nodes was smaller than 10 mm (5.77 ± 1.81 mm, range 3.7–9 mm), which is the standard cut-off reported in the literature for pelvic lymph nodes [15,16].

To the best of our knowledge, no other study has so far specifically tackled the issue of nodal staging in prostate cancer by means of DWI using fitted ADC measurements obtained from a multiple *b* value DWI sequence. This kind of evaluation overcomes the problem of choosing a specific *b* value for ADC measurements, because fitted ADC are calculated on the basis of a logarithmic curve obtained with multiple *b* values. Moreover, the usage of a higher magnetic field strength (3.0 T versus 1.5 T) should be advantageous as it can provide higher spatial resolution and signal-to-noise ratio.

However, to maximize accuracy in MRI-based lymph node staging, it is important to be aware of the following potential pitfalls of DWI:

1. Small nodes (<4 mm in long axis diameter) may be displayed and anatomically localised using DWI, but the presence of malignant disease cannot always be established based on the sole DWI findings;
2. ADC measurements in normal-sized lymph nodes may be degraded by partial volume effects;
3. Necrosis inside metastatic nodes may lead to false-negative results due to the resultant ADC increase, and therefore macroscopic areas of intranodal necrosis must be carefully discarded;
4. Any reactive changes in lymph nodes may result in lower ADC values;
5. Technical factors such as image noise and motion artefacts can lead to systematic or random errors in ADC quantification;
6. Micrometastases in smaller lymph nodes with insufficient intranodal tumor burden may not impede water diffusion and can therefore lead to false-negative results [4].

Besides, our study has several limitations. First, the number of patients (and in particular, of those with malignant lymph nodes) was relatively low. Second, we excluded from image analysis all lymph nodes smaller than 5 mm in their maximum diameter, which still could be malignant in nature. Third, a station-by-station instead of a node-by-node analysis was performed. Nevertheless, surgical specimens often included multiple lymph nodes, so it was not possible to have a 100% pathological correlation at each single lymph node level, especially in the case of multiple lymph nodes at a single nodal station.

In conclusion, our preliminary experience suggests that 3.0 T SE-EPI diffusion-weighted MR imaging with multiple *b* values may help distinguish benign from malignant pelvic lymph nodes in patients with prostate cancer. In particular, fitted ADC measurements could represent a useful method in this differential diagnosis when using a threshold value of 0.91×10^{-3} mm^2/s. Since DWI requires only a very short prolongation of the standard MRI examination protocol, this technique could be recommended as part of a routine MRI study of the pelvis as an additional tool for characterisation of pelvic lymph nodes. However, further studies with a larger patient sample are necessary to confirm our findings.

Conflict of interest

None.

References

[1] A. Heidenreich, J. Bellmunt, M. Bolla, et al., EAU guidelines on prostate cancer. Part 1: screening, diagnosis and treatment of clinically localised disease, Eur. Urol. 59 (2011) 61–71.
[2] A. Briganti, F.K.-H. Chun, A. Salonia, et al., Validation of a nomogram predicting the probability of lymph node invasion among patients undergoing radical prostatectomy and extended pelvic lymphadenectomy, Eur. Urol. 49 (2006) 1019–1027.
[3] A. Briganti, How to improve the ability to detect pelvic lymph node metastases of urologic malignancies, Eur. Urol. 55 (2009) 770–772.
[4] A.L. Baert, M.F. Reiser, H. Hricak, M. Knauth, D.M. Koh, H.C. Thoeny, Diffusion Weighted MR Imaging. Applications in the Body, Springer-Verlag, Berlin, Heidelberg, 2010.
[5] M.F. Bellin, L. Lebleu, J.B. Meric, et al., Evaluation of retroperitoneal and pelvic lymph node metastases with MRI and MR lymphography, Abdom. Imaging 28 (2003) 155–163.
[6] A.A. Abdel Razek, S. Elkammary, A.S. Elmorsy, M. Elshafey, T. Elhadedy, Characterization of mediastinal lymphadenopathy with diffusion-weighted imaging, Magn. Reson. Imaging 29 (2011) 167–172.
[7] F.C. Burkhard, M.C. Schumacher, U.E. Studer, An extended pelvic lymph node dissection should be performed in most patients if radical prostatectomy is truly indicated, Nat. Clin. Pract. Urol. 3 (2006) 454–455.
[8] C.M. Tempany, B.J. McNeil, Advances in biomedical imaging, JAMA 285 (2001) 562–567.
[9] S. Katz, M. Rosen, MR imaging and MR spectroscopy in prostate cancer management, Radiol. Clin. N. Am. 44 (2006) 723–734.
[10] M.C. Schumacher, F.C. Burkhard, G.N. Thalmann, A. Fleischmann, U.E. Studer, Good outcome for patients with few lymph node metastases after radical retropubic prostatectomy, Eur. Urol. 54 (2008) 344–352.
[11] H.C. Thoeny, M. Triantafyllou, F.D. Birkhaeuser, et al., Combined ultrasmall superparamagnetic particles of iron oxide-enhanced and diffusion-weighted magnetic resonance imaging reliably detect pelvic lymph node metastases in normal-sized nodes of bladder and prostate cancer patients, Eur. Urol. 55 (2009) 761–769.
[12] M.G. Harisinghani, J. Barentsz, P.F. Hahn, et al., Noninvasive detection of clinically occult lymph-node metastases in prostate cancer, N. Engl. J. Med. 348 (2003) 2491–2499.
[13] C. Roy, G. Bierry, A. Matau, et al., Value of diffusion-weighted imaging to detect small malignant pelvic lymph nodes at 3 T, Eur. Radiol. 20 (2010) 1803–1811.
[14] S.H. Warncke, A. Mattei, F.G. Fuechsel, S. Z'Brun, T. Krause, U.E. Studer, Detection rate and operating time required for gamma probe-guided sentinel lymph node resection after injection of technetium-99 m nanocolloid into the prostate with and without preoperative imaging, Eur. Urol. 52 (2007) 126–132.
[15] G. Giannarini, G. Petralia, H.C. Thoeny, Potential and limitations of diffusion-weighted magnetic resonance imaging in kidney, prostate, and bladder cancer including pelvic lymph node staging: a critical analysis of the literature, Eur. Urol. 61 (2012) 326–340.
[16] S.J. Vinnicombe, A.R. Norman, V. Nicolson, J.E. Husband, Normal pelvic lymph nodes: evaluation with CT after bipedal lymphangiography, Radiology 194 (1995) 349–355.